Journal of the Mechanics and Physics of Solids 133 (2019) 103737

Contents lists available at ScienceDirect

Journal of the Mechanics and Physics of Solids

journal homepage: www.elsevier.com/locate/jmps

Polyacrylamide hydrogels. II. elastic dissipater

Junjie Liu[a,b], Canhui Yang[a,c], Tenghao Yin[a,b], Zhengjin Wang[a,d], Shaoxing Qu[b], Zhigang Suo[a,*]

[a] John A. Paulson School of Engineering and Applied Sciences, Kavli Institute for Bionano Science and Technology, Harvard University, MA 02138, USA

[b] State Key Laboratory of Fluid Power & Mechatronic System, Key Laboratory of Soft Machines and Smart Devices of Zhejiang Province, Department of Engineering Mechanics and Center for X-Mechanics, Zhejiang University, Hangzhou 310027, China

[c] Department of Mechanics and Aerospace Engineering, Southern University of Science and Technology, Shenzhen, Guangdong 518055, China

[d] State Key Laboratory for Strength and Vibration of Mechanical Structures, School of Aerospace Engineering, Xi'an Jiaotong University, Xi'an 710049, China

ARTICLE INFO

Article history:
Received 24 July 2019
Revised 3 September 2019
Accepted 18 September 2019
Available online 18 September 2019

Keywords:
Peel
Hydrogel
Polyacrylamide
Size-dependent toughness
Elastic dissipater

ABSTRACT

A rubber band is an elastic dissipater. It has narrow hysteresis on load and unload, but dissipates all its elastic energy on snap. We hypothesize that the dissipation of elastic energy can be a potent toughening mechanism. A polyacrylamide hydrogel has narrow hysteresis, but appreciable toughness, providing an ideal candidate to test the hypothesis of elastic dissipater. We peel the polyacrylamide hydrogel of various thicknesses, and record the steady peel forces. A transition thickness exists, below which the steady peel force increases linearly with thickness, and above which the steady peel force is independent of thickness. The transition thickness is comparable to the fractocohesive length, defined by the ratio of toughness over the work of fracture, and is ~1 mm for the polyacrylamide hydrogel. The linear slope is comparable to the work of fracture. The linear extrapolation of the steady peel force to vanishing thickness defines the peel threshold, and the thickness-independent steady peel force defines the toughness. The former is much below the latter. We interpret these experimental findings in terms of elastic dissipater. A crack not only cuts a layer of polymer chains, but also breaks some polymer chains in a zone of thickness comparable to the fractocohesive length. Even though only a small fraction of the chains in the zone rupture, all the elastic energy stored in this zone dissipates and contributes to toughness. The entire zone acts as an elastic dissipater, not just a layer of individual polymer chains. We discuss the importance of the elastic dissipater in creating materials of high toughness, high threshold, and low hysteresis.

1. Introduction

The resistance to the growth of a crack in a polymer network of entropic elasticity has long been interpreted using the Lake-Thomas model (Lake and Thomas, 1967). The model represents the following picture. Monomers link into polymer chains by covalent bonds, and the polymer chains crosslink into a network also by covalent bonds. Except at the crosslinks, the polymer chains interact through noncovalent bonds, which are negligibly weak compared to the covalent bonds. This

* Corresponding author.
E-mail address: suo@seas.harvard.edu (Z. Suo).

https://doi.org/10.1016/j.jmps.2019.103737
0022-5096/

mix of covalent and noncovalent bonds is essential to both the elasticity and rupture of the network. At the crack front, just before a polymer chain ruptures, all covalent bonds in the polymer chain are stretched near the limit. The rupture of the polymer chain breaks only one covalent bond in the polymer chain, but dissipates the elastic energy stored in all bonds in the polymer chain. The polymer chains off the crack plane do not dissipate energy. The energy needed to create unit area of crack is $\Gamma_o = \alpha l\sqrt{n}J/V$, where J is the energy per covalent bond along the polymer chain, V the volume of a monomer, l the length of a monomer, n the number of monomers along a polymer chain, and α a dimensionless number of order of unity. In the Lake-Thomas model, each polymer chain at the crack front is an elastic dissipater.

Lake and Thomas identified their prediction to the fatigue threshold, below which a crack does not grow in an elastomer under cyclic load. Natural rubber, for instance, has toughness above 10,000 J/m^2 under monotonic load, but threshold below 100 J/m^2 under cyclic load. Under a monotonic load, as the crack cuts a layer of polymer chains, the elastomer in a zone off the crack plane also dissipates energy by inelastic processes, such as stretch-induced crystallization, viscoelasticity, and polymer-filler interaction. The thickness of the inelastic zone is much larger than the mesh size of the polymer network. The picture is analogous to that of a metal (Irwin, 1948; Orowan, 1950). Under a cyclic load, just above the threshold, the crack can cut a layer of polymer chains without activating the inelastic processes in the elastomer off the crack plane.

More recently, advances have taken place in developing tough entropic polymer networks not only for elastomers, but also for hydrogels, ionogels, and organogels (Gong et al., 2003; Gong, 2010; Sun et al., 2012; Creton, 2017). These discoveries in materials have rekindled broad interest in fracture of polymer networks (Kundu and Crosby, 2009; Wang and Hong, 2012; Zhao, 2014; Zhang et al., 2015; Long and Hui, 2015, 2016; Creton and Ciccotti, 2016; Noselli et al., 2016; Mao et al., 2017; Mao and Anand, 2018; Naassaoui et al., 2018; Yu et al., 2018; Bai et al., 2019b). In particular, the Lake-Thomas model has also explained the threshold in tough hydrogels under cyclic loads, but with an interesting twist (Bai et al., 2017; Zhang et al., 2018b, 2019; Zhou et al., 2019). A tough hydrogel contains two polymer networks: one network contributes to the threshold, and the other network only contributes to the toughness.

A previous paper (Chen et al., 2017) and Paper I of this series (Yang et al., 2019) have reported an enormous difference in fractocohesive length, defined by $R_f = \Gamma/W_f$, where Γ is the toughness measured by stretching a sample with a cut, and W_f is the work of fracture measured by stretching a sample without cut. We have tested a polyacrylamide hydrogel under the conditions that minimize the effect of time-dependent inelastic processes such as viscoelasticity and poroelasticity. For a sample with a cut of some length, the rupture stretch is unaffected if the cut is short, but is reduced if the cut is long. The transition cut length, or the flaw sensitivity length, is comparable to the fractocohesive length. The Lake-Thomas model predicts that the fractocohesive length is on the order of the mesh size of the polymer network, about 10 nm, but the experimentally determined fractocohesive length of the hydrogel is on the order of 1 mm.

We have reconciled this difference as follows. For a perfect, entropic polymer network, the toughness is estimated by the Lake-Thomas model, $\Gamma = \Gamma_o = \alpha l\sqrt{n}J/V$, and the work of fracture is estimated by the covalent energy per volume, $W_f = J/V$. Their ratio gives the fractocohesive length on the order of mesh size of the network, $l\sqrt{n}$. A real polyacrylamide hydrogel has an imperfect network (Yang et al., 2019). The crack not only cuts a layer of polymer chains on the crack plane, but also breaks some of the polymer chains off the crack plane, so that the toughness much exceeds the Lake-Thomas prediction. For a sample without cut, the network imperfection greatly reduces the work of fracture. The two effects—increased toughness and reduced work of fracture—in combination give a fractocohesive length of 1 mm.

Here we focus on another discrepancy between theory and experiment exposed in Paper I. The polyacrylamide hydrogel has narrow hysteresis, but appreciable toughness. The measured toughness is more than one order of magnitude higher than the Lake-Thomas prediction. We hypothesize that the entire zone, of the thickness of the fractocohesive length, acts as an elastic dissipater, not just a layer of individual polymer chains. We test this hypothesis by peeling the polyacrylamide hydrogel of various thicknesses. The large fractocohesive length of 1 mm readily allows us to peel hydrogels of thicknesses both below and above the fractocohesive length. We review the mechanics of peel (Section 2) and describe experimental methods (Section 3). Fig. 1 summarizes the main experimental findings (Section 4). The steady peel force (per unit width of the hydrogel) depends on hydrogel thickness. A transition thickness is noted, below which steady peel force is linear in the thickness, and above which steady peel force is independent of the thickness. The linear extrapolation of the steady peel force to vanishing thickness defines the peel threshold, corresponding to the Lake-Thomas prediction (Section 5). The transition thickness is comparable to the fractocohesive length (Section 6). The slope of the line is comparable to the work of fracture, which is about one order of magnitude higher than the hysteresis energy (Section 7). That is, all the elastic energy stored in the fracture process zone contributes to fracture toughness, even though only a small fraction of the polymer chains in this zone rupture (Section 8). We discuss the importance of the elastic dissipater in creating materials of high toughness, high threshold, and low hysteresis.

2. The mechanics of peel

Peel is a common test of soft materials (Gent, 1974; Gent and Hamed, 1977). Here we peel a layer of a polyacrylamide hydrogel, thickness h and width w, sandwiched between a rigid substrate and an inextensible backing tape (Fig. 2). As the machine pulls the tape at a constant velocity v, a motor moves the substrate horizontally at the same velocity, so that the peeled sample always remains perpendicular to the substrate. A force sensor records the peel force F. When the machine pulls the tape by a distance dz, the force does work Fdz, the elastic energy of the hydrogel changes by dU, the crack extends by length dc, and the energy release rate G is defined by $Fdz = dU + Gwdc$ (Rivlin and Thomas, 1953). As the pull distance

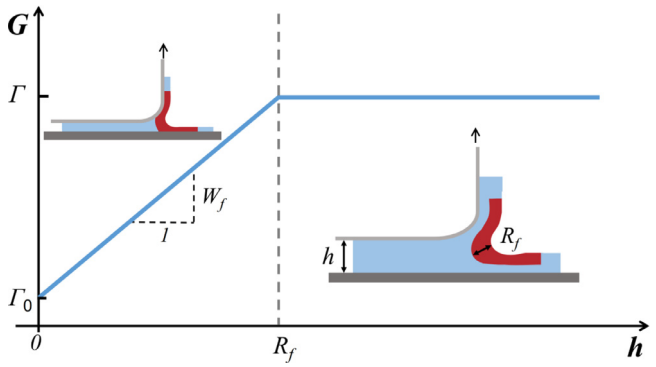

Fig. 1. Steady peel force, G, depends on the hydrogel thickness, h. The G-h relation is characterized by four quantities: peel threshold Γ_0, toughness Γ, work of fracture W_f, and transition thickness R_f. The insets illustrate a hydrogel, thickness h, sandwiched between a rigid substrate and an inextensible tape, and peeled by a force. Highlighted in each inset is the zone of energy dissipation (i.e., the fracture process zone). When the hydrogel thickness is below the transition thickness, $h < R_f$, the entire thickness of the hydrogel dissipates energy, and the steady peel force is linear in the thickness, $G = \Gamma_0 + hW_f$. When the hydrogel thickness is above the transition thickness, $h > R_f$, only a part of the thickness of the hydrogel dissipates energy, and the steady peel force reaches the toughness Γ.

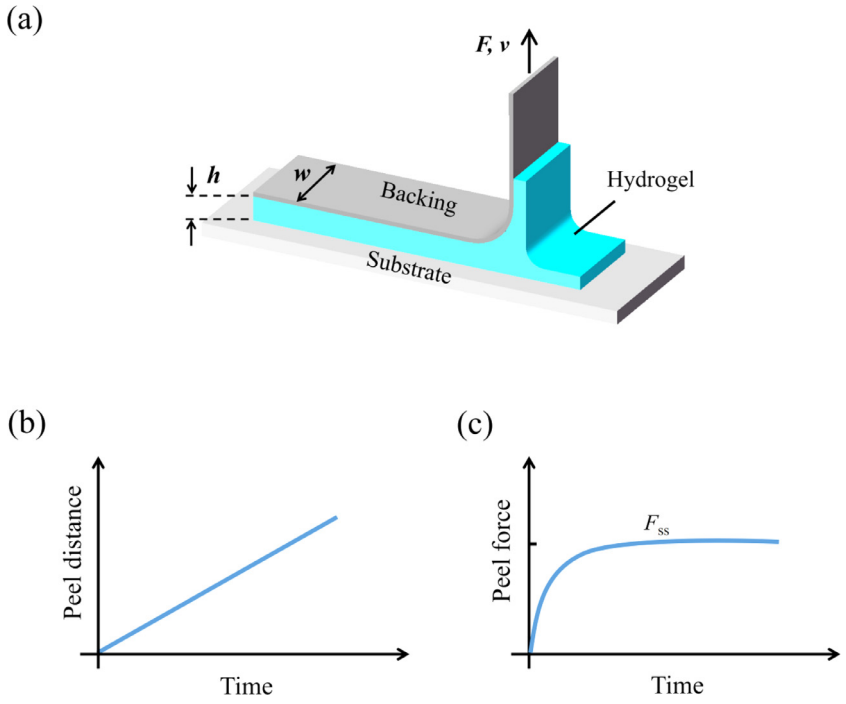

Fig. 2. Peel test. (a) Experimental setup. (b) A loading machine prescribes the peel distance linear in time. (c) A force sensor records the peel force as a function of time.

increases, the crack initially blunts but does not extend, and the applied force F increases with the pull distance z. Then the crack extends and the peel force reaches a steady state, F_{ss}. In the steady state, because the backing tape is inextensible, the increment in the pull distance equals the extension of the crack, $dz = dc$. In the steady state, the active zone of deformation translates with the crack front, and the elastic energy in the hydrogel is invariant, $dU = 0$. Inserting these steady state conditions into the equation that defines the energy release rate, one obtains that $G = F_{ss}/w$.

As the crack front advances, a material particle undergoes a history of loading and unloading (Bai et al., 2019a). Imagine three material particles marked beside the crack path (Fig. 3). Particle A is far ahead of the crack front and has not deformed. Particle B is close to the crack front and is being stretched. Particle C is far behind of the crack front and is unloaded. As the crack front advances, a material particle experiences sequentially the undeformed state, the highly stretched state, and the unloaded state. As the crack extends in the steady velocity v, the zone of active deformation translates at the same velocity, and the size of the zone scales with the thickness of the hydrogel, h. Consequently, the time of the active deformation of every material particle is estimated by h/v.

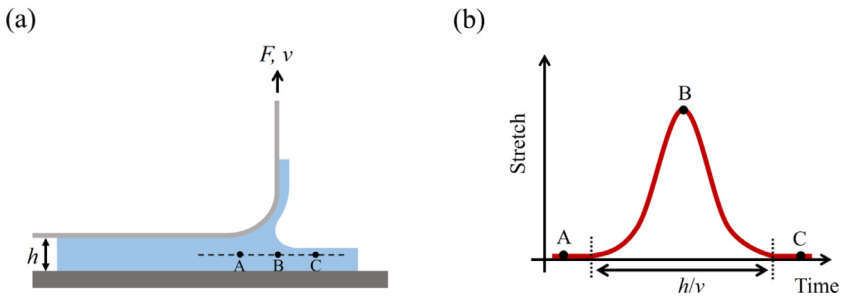

Fig. 3. Time scale of active deformation. (a) Three material particles are marked beside the crack path. (b) Deformation history of a material particle during steady peel. The time of active deformation scales as h/v.

Time-dependent inelastic processes, such as poroelasticity and viscoelasticity, are of great interest by themselves, but they confound with the thickness effect; see a recent paper on hearing a hydrogel of complex rheology (Bai et al., 2019a). In designing our peel experiment, we have chosen conditions that minimize the effects of time-dependent inelastic processes. For all peel tests reported in this paper, we keep the time of active deformation constant, $h/v = 0.6$ s. At this time scale, the relevant length scale of poroelasticity is $\sqrt{Dt}$, where D is the effective diffusivity of water in the polyacrylamide hydrogel, and t is the diffusive time. Given $D \sim 10^{-10}$ m^2/s (Kalcioglu et al., 2012) and $t \sim 0.6$ s, we estimate the diffusion length to be on the order of 10 μm, which is much smaller than the thickness of the thinnest hydrogel in our experiment, 250 μm. Polyacrylamide hydrogel also has low viscoelasticity (Zhang et al., 2018a). The stress-stretch curves of polyacrylamide hydrogel show little difference even though the applied stretch rate ranges from 1/s to 0.05/s (Yang et al., 2019). In unpublished experiments, we find that the steady peel force varies within a factor of 3 when the time scale h/v spans four orders of magnitude, from 0.15 to 1500 s. In such experiments, we use oil to avoid the water loss of the hydrogel in long time test, and show that the effect of viscoelasticity is small.

3. Experimental methods

We purchase monomer acrylamide (AAm, A8887), crosslinker N,N′-methylenebisacrylamide (MBAA, M7279), photoinitiator 2-Hydroxy-4′-(2-hydroxyethoxy)-2-methylpropiophenone (Irgacure-2959, 410896), ethyl alcohol (CH_3CH_2OH, 459844), 3-(trimethoxysilyl) propyl methacrylate (TMSPMA, 440159), and acetic acid (A6283) from Sigma Aldrich. We purchase polyester (PET) films, acrylic sheets, and cyanoacrylate adhesive (Krazy glue) from McMaster-Carr. We purchase silica glass slides and isopropyl alcohol (IPA, BDH1174) from VWR. We purchase deionized water (DI water) from Poland Spring. All chemicals are used as received.

We wash a glass slide with the IPA and DI water twice, and then dry the washed glass slide by air. The clean surface of the clean glass slide has abundant hydroxyl groups (Fig. 4a). Then we prepare silane solution. For 100 ml of deionized water, 10 μl acetic acid and 2 ml TMSPMA are added. The mixture is vigorously stirred for 1 min. The clean glass is immersed into the silane solution for 2 h. During the soaking, the silanes hydrolyze into silanol groups, and condensate into siloxane bonds with the hydroxyl groups on the glass surface (Yuk et al., 2016) (Fig. 4b). After soaking, the glass substrate is washed by the ethyl alcohol, followed by air drying.

Subsequently, we prepare hydrogel precursor. For every 86 ml of deionized water, 14 g AAm, 0.0085 g MBAA and 150 μl I-2959 solution (0.1 M in ethyl alcohol) are added. The hydrogel precursor is cast on the silane modified glass slide with a rigid mold, covered by an untreated glass, and illuminated under a UV lamp (15 W, 365 nm, UVP XX-15 L) for 1 h (Fig. 4c). We use different molds to cast hydrogel precursor with various thicknesses. The molds have engraved rectangle with 20 mm in width and 70 mm in length, while the thickness varies from 250 μm to 4.5 mm. We use the PET films to make the molds of thickness below 1 mm and use the acrylic sheets to make the molds of other thickness. After curing, the polyacrylamide hydrogel adheres through the siloxane bonds to the glass substrate on the bottom. We disassemble the mold and glass cover, bond a PET tape with thickness of 50 μm on the top of the hydrogel using cyanoacrylate, and introduce a precut of length ~5 mm between hydrogel and glass by a razor blade.

Finally, the sample is loaded to a mechanical testing machine (Instron 5966). As the machine pulls the PET tape vertically at a constant velocity v, a motor moves the substrate horizontally at the same velocity, so that the peeled sample always remains perpendicular to the substrate (Fig. 4d). In peeling hydrogels of various thicknesses, we keep the time scale of active deformation fixed at $h/v = 0.6$ s.

We also measure stress-stretch curves using large thin sheets of the hydrogel without precut crack. We use the above recipe to synthesize thin sheets of the polyacrylamide hydrogel, thickness 1.5 mm, width 100 mm, and height 40 mm. We glue the two wide edges of the sheet to acrylic sheets using cyanoacrylate. The gage length of the hydrogel is 6 mm. We load a sample monotonically to rupture, and record the nominal stress as a function of the stretch. The area underneath the stress-stretch curve up to rupture gives the work of fracture, W_f. We load another sheet to a stretch of 10, which is close to the rupture stretch, and unload the sample. The area enclosed by the loading curve and the unloading curve represents the

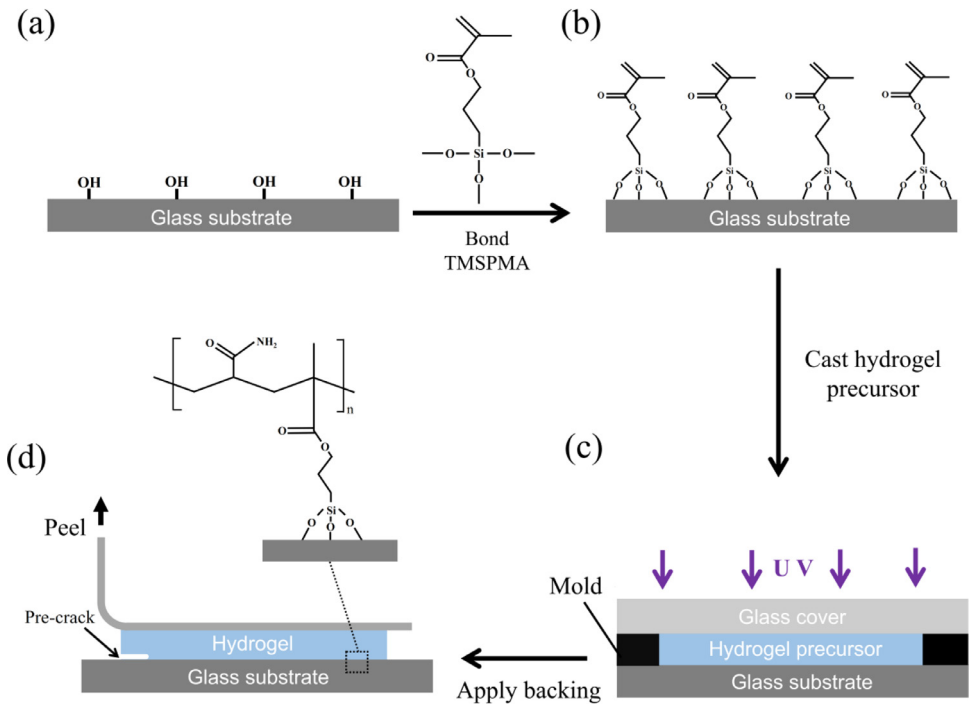

Fig. 4. Sample preparation. (a) The surface of a clean glass substrate is rich in hydroxyl groups. (b) Silane functional groups are chemically anchored on the glass substrate through the condensation between silanol groups and hydroxyl groups. (c) Polyacrylamide hydrogel precursor is cast on the silane-modified glass substrate, sealed by an untreated glass cover and exposed to UV for 1 h. The thickness of the hydrogel is controlled by the mold used. (d) After curing, the polyacrylamide hydrogel is chemically bonded to the glass substrate. A PET tape is bonded on the top surface of the hydrogel using cyanoacrylate. A precrack between hydrogel and glass substrate is made using a razor blade.

hysteresis energy, W_D. The loading speed is fixed at 10 mm/s, so that the time scale—the gage length divided by the loading speed—is the same as the time scale of active deformation in the peel test, 0.6 s.

4. Experimental results

During peel, the precrack on the hydrogel/substrate interface kinks into the hydrogel, resulting in cohesive failure (Fig. 5). After peel, hydrogel residues are observed on both the backing tape and the substrate.

We measure the force-displacement curves of the hydrogel of thicknesses 0.25 mm, 0.5 mm, 0.75 mm, 1.0 mm, 1.5 mm, 3.0 mm, and 4.5 mm, using at least three samples for each thickness (Fig. 6). In each peel, the peel force increases with the peel displacement initially, and then plateaus. The beginning of plateau is set to be right after the first drop of the peel force, and the termination of plateau is set to be right before the complete peel-off of the hydrogel. The "plateau force" fluctuates. Such stick-slip is often observed in peeling and tearing rubbery materials, indicative of a negative slope of the force as a function of velocity (Gardon, 1963; Greensmith and Thomas, 1955; Webb and Alfantis, 1995). The stick-slip is ascribed to time dependent toughening, such as crystallization (Greensmith and Thomas, 1955), viscoelasticity (Gent and Petrich, 1969), and poroelasticity (Tanaka et al., 2009). Pursuing these kinetic effects is beyond the scope of the current paper. Here we follow a common practice: define the steady state peel force, F_{ss}, by averaging the plateau force over the peel displacement, and calculate the energy release rate by the steady state peel force per unit width, $G = F_{ss}/w$.

We plot the steady peel force per unit width (i.e., the energy release rate), G, as a function of the thickness of polyacrylamide hydrogel, h (Fig. 7). We sketch two dashed lines to guide the eye. A transition thickness, ~1 mm, exists. When the hydrogel is thinner than the transition thickness, the steady peel force is linear in the thickness at a slope of $\sim 1.87 \times 10^5\,\mathrm{J/m^3}$. The linear extrapolation of the steady peel force to vanishing thickness defines the peel threshold, $\sim 7.9\,\mathrm{J/m^2}$. When the hydrogel is thicker than the transition thickness, the steady peel force is independent of the thickness and plateaus at $\sim 163.5\,\mathrm{J/m^2}$.

5. Peel threshold

According to the Lake-Thomas picture, in the absence of inelastic dissipation in the bulk, the energy needed to advance a unit area of a crack equals the covalent energy in a single layer of polymer chains (Lake and Thomas, 1967). In peel, steady peel force extrapolated to vanishing thickness defines the peel threshold. We expect that the peel threshold corresponds to

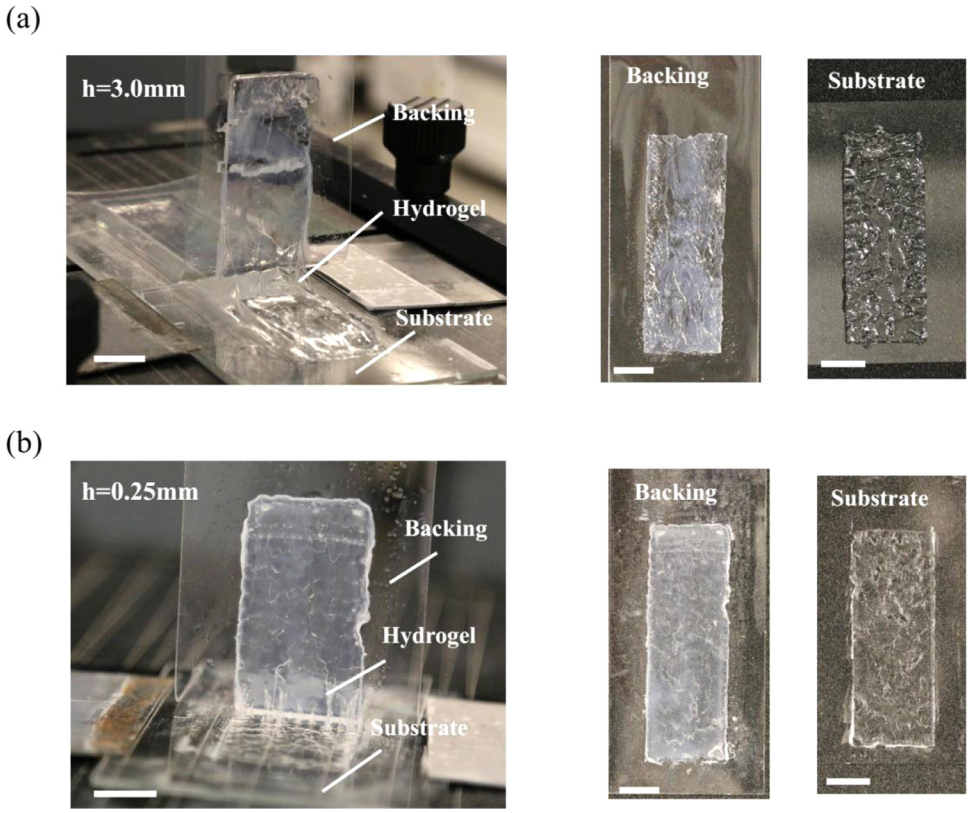

Fig. 5. (a) A hydrogel, thickness 3 mm, is peeled at a velocity of 5 mm/s. (b) A hydrogel, thickness 0.25 mm, is peeled at a velocity of 0.42 mm/s. In both cases, the crack advances inside the hydrogel, rather than on the hydrogel/glass interface or the hydrogel/PET interface. After peel, hydrogel residues are observed on both the backing tape and the substrate. The scale bars represent 1 cm.

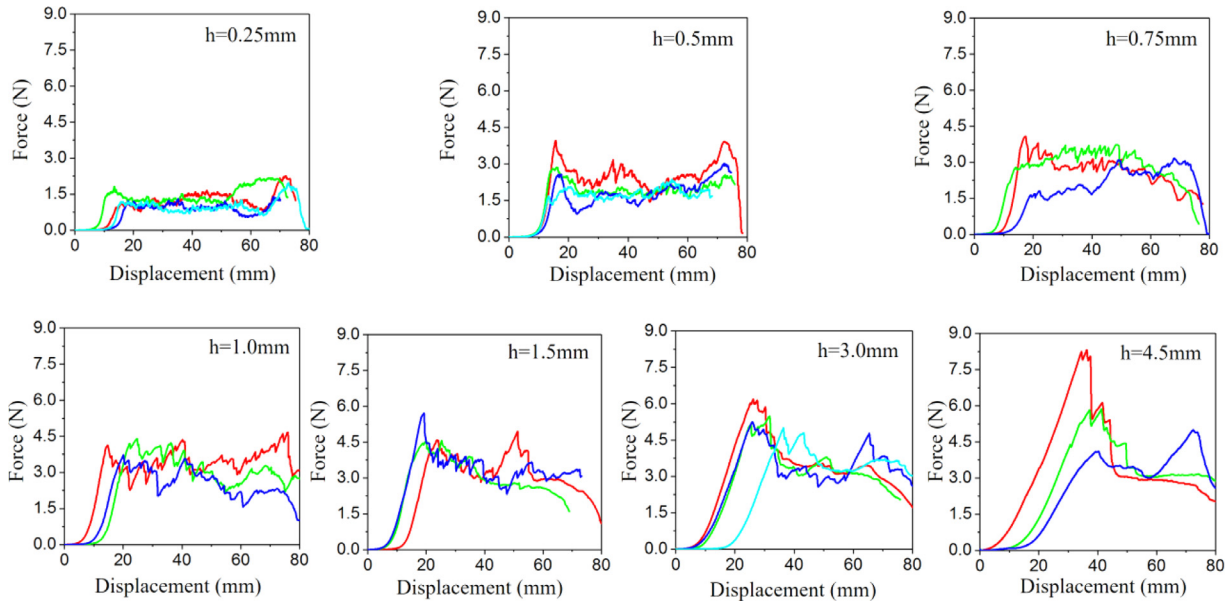

Fig. 6. Force-displacement curves of the hydrogel of various thicknesses. The time scale h/v is kept as a constant of 0.6 s.

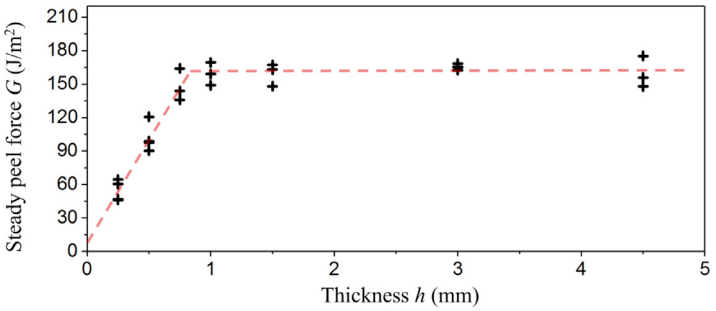

Fig. 7. Experimentally determined steady peel force, G, as a function of hydrogel thickness, h. The black plus signs are experimental data. The two dashed lines are drawn to guide the eye. The G-h relation is characterized by four quantities: the transition thickness ~1 mm, the slope 1.87×10^5 J/m^3, the plateau ~163.5 J/m^2, and the peel threshold ~7.9 J/m^2.

the Lake-Thomas limit. We estimate the Lake-Thomas limit by $\Gamma_0 = \phi l \sqrt{n} J/V$, where ϕ is the volume fraction of the polymer in hydrogel, n the number of monomers in a polymer chain, l the length of a monomer, J the covalent energy of a carbon-carbon bond, and V the volume of a monomer. Our recipe gives $n \sim 1786$, $\phi \sim 12.8\%$, $l \sim 4.6 \times 10^{-10}$ m, $V \sim 10^{-28}$ m^3. Taking $J \sim 4.6 \times 10^{-10}$ J (Luo, 2007), we get theoretical value $\Gamma_0 \sim 12.4$ J/m^2, which is comparable to the experimental value, 7.9 J/m^2.

The peel threshold has rarely been reported in the literature, and has been interpreted as surface energy (Igarashi, 1975). This interpretation is inappropriate for our experiment. The surface energy of a polyacrylamide hydrogel (with about 90% of water) is on the order of 10^{-1} J/m^2, smaller than the experimental measurement by two orders of magnitude. The discrepancy is readily understood. The surface energy originates from noncovalent intermolecular interaction, which is weak. By contrast, peel breaks the covalent bonds in the hydrogel network, which is strong.

The peel threshold determined here is comparable to the fatigue threshold previously reported for polyacrylamide hydrogels (Bai et al., 2019b; Tang et al., 2017; Zhang et al., 2018a, 2019). Recall the real polymer network of polyacrylamide hydrogel has distributed chain length and is imperfect. Under monotonic load, the scission of short chains in the bulk hydrogel acts as a solid-like toughener and amplifies the toughness of polyacrylamide hydrogel. Under cyclic load, however, the scission of short chains in the bulk can occur in previous cycles and does not contribute to the threshold. The Lake-Thomas limit estimates both the peel threshold and fatigue threshold. The peel threshold is a proxy for the fatigue threshold. This proxy is of practical significance, because the direct measurement of the fatigue threshold is time-consuming, requiring many load cycles.

6. Transition thickness

The steady peel force switches from being thickness-dependent to being thickness-independent at a transition thickness ~1 mm. In peel of soft materials, the measurement of the transition thickness is often challenging since both the peel velocity and temperature profoundly affect steady peel force (Gent and Petrich, 1969). Furthermore, the failure mode can change from cohesive mode to adhesive mode (Aubrey et al., 1969). Such complications are minimized in peeling the polyacrylamide hydrogel. In our experiments, cohesive failure is observed in all samples. Within the test conditions used here, the steady peel force changes within a factor of 3 when the peel velocity changes by orders of magnitude.

The fractocohesive length is defined by $R_f = \Gamma / W_f$, where Γ is the toughness measured using samples with precut crack, and W_f is the work of fracture measured using samples without precut crack (Chen et al., 2017). The fractocohesive length is material-specific, and scales several other lengths. First, when the fracture process zone is small compared with the characteristic length of the sample, the fractocohesive length scales the size of the fracture process zone. Second, for a large sheet containing a cut of some length, the rupture stretch is unaffected if the cut is short, but is reduced if the cut is long; the transition cut length scales with the fractocohesive length. Third, the peel data reported here show that the transition thickness in the G-h relation is comparable to the fractocohesive length. When the hydrogel is thick, the steady peal force is independent of the hydrogel thickness, and is taken to be the toughness, $\Gamma = 163.5$ J/m^2. The work of fracture, as determined in the next section, is $W_f = 1.51 \times 10^5$ J/m^3. Thus, the fractocohesive length is $R_f = 1.1$ mm, which is comparable to the transition thickness in the G-h relation (Fig. 7).

Recall that a hydrogel network is imperfect. When the effect of viscoelasticity and poroelasticity is minimized, inelastic deformation occurs due to the scission of short chains. When the thickness of the hydrogel is smaller than the fractocohesive length, the inelastic deformation is localized around the crack front with a volume scaling as $h^2 w$, so that the steady peel force increases with the thickness of the hydrogel. When the thickness of the hydrogel is larger than the fractocohesive length, the volume of inelastic zone becomes a constant, $R_f^2 w$, the steady peel force is independent of the thickness of the hydrogel.

Also note that, in Paper I, we stretched thin sheets containing long cuts, giving toughness $\Gamma = 515.7$ J/m^2. This value is considerably larger than the toughness determined is the current paper by peeling the hydrogel, $\Gamma = 163.5$ J/m^2. Note

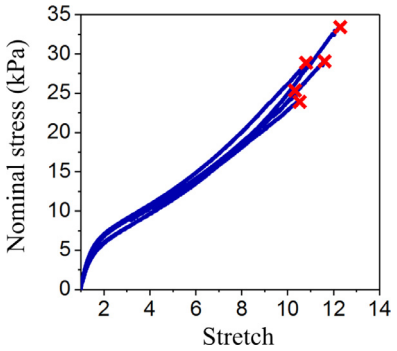

Fig. 8. Five thin sheets of the hydrogel are pulled to rupture. Nominal stress is measured as a function of stretch. The red crosses indicate rupture.

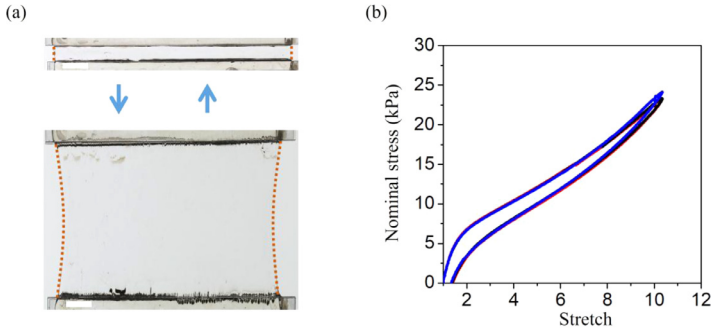

Fig. 9. (a) Images showing a hydrogel subject to load and unload with a maximum stretch of 10. The scale bars represent 1 cm. The dashed line indicates the profile of the hydrogel. (b) Nominal stress is measured as a function of stretch. The results of three samples are plotted.

that the two works have used the hydrogel of the same recipe. Perhaps the difference is unsurprising, given that the crack front in the thin sheet deforms under the plane stress conditions, whereas the crack front in peel deforms under the plane strain conditions. Similar difference has been reported in ductile metals, and is caused by plasticity in different types of deformation. However, the hydrogel does not undergo plastic deformation; we refrain from further speculation here before a more systematic study of this difference.

7. Work of fracture W_f and hysteresis energy W_D

The slope in the linear range of the *G*-*h* relation has the unit of energy per volume, J/m^3. Previous experiments have shown that the slope is approximately the hysteresis energy per unit volume, W_D, with the maximum stretch close to rupture (Gent and Hamed, 1977; Igarashi, 1975). For polyacrylamide hydrogel, the hysteresis energy is much smaller than the work of fracture, $W_D << W_f$, indicating that only small fraction of chains break during fracture. Here we separately measure the hysteresis energy W_D and work of fracture W_f by stretching thin sheets of the hydrogel without precut crack. Each thin sheet is a long rectangle, width 100 mm and height 6 mm. The wide edges of the sheet are glued to rigid plastics, which are the pulled in the direction of height. We select this setup to measure stress-stretch curves because the type of deformation is similar to that of the peel front, where the rigid substrate and inextensible tape suppress the stretch in the width of the hydrogel, allow the stretch in the direction of the thickness, and keep the surface of the front traction-free.

We pull the thin sheet of the hydrogel up to rupture, and record the nominal stress as a function of stretch (Fig. 8). Five samples synthesized from different benches are tested. The average rupture stretch is determined as 11.08 ± 0.82. The work of fracture, calculated by the area beneath the stress-stretch curve to rupture, is $W_f = (1.51 \pm 0.23) \times 10^5$ J/m^3. As discussed in Paper I, the statistical scatters of the rupture properties of the hydrogel are much smaller than those commonly observed in hard elastic materials, such as inorganic glass and ceramics (Yang et al., 2019).

We then load and unload a thin sheet without precut crack with a maximum stretch of 10, which is close to ultimate stretch, and record the nominal stress as a function of stretch (Fig. 9). The area enclosed by the loading-unloading curve is the hysteresis energy W_D during that loading cycle. Similar to the observation reported in Paper I, the hysteresis energy of polyacrylamide hydrogels is small. The average hysteresis energy is $W_D \sim (2.15 \pm 0.08) \times 10^4$ J/m^3. This value is smaller than the slope determined in the peel test, 1.87×10^5 J/m^3, by one order of magnitude. Thus, the hypothesis that the slope is estimated by W_D is invalid for the polyacrylamide hydrogel.

For the polyacrylamide hydrogel reported here, the area enclosed by the loading-unloading curve only makes up for about 14% of the area under the loading curve. By contrast, for the peel of viscous adhesives, the hysteresis energy makes

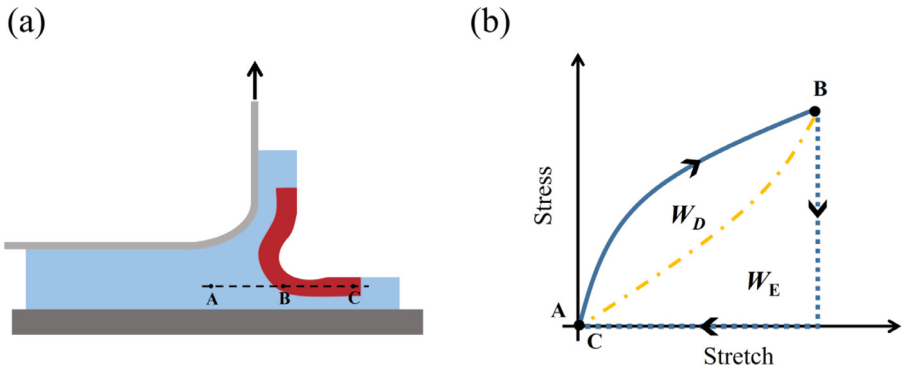

Fig. 10. Generalized Lake-Thomas model. (a) Imagine three material particles marked beneath the crack path. Particle A is far ahead of the crack front and has not deformed. Particle B is close to the crack front and is highly stretched. Particle C is far behind of the crack front and is unloaded. (b) For a large thin sheet subject to load and unload up to a point near rupture, the loading and unloading curves define two areas: the elastic energy W_E, and the hysteresis energy W_D. The material particle has not deformed at point A, loaded to point B near fracture, and unloaded to point C. For a large thin sheet subject to a load all the way to rupture, however, the entire area under the loading curve is dissipated, so that the work of fracture is $W_f = W_E + W_D$.

up for the vast majority of work of fracture (Igarashi, 1975). For double-network hydrogels, the toughness linearly depends on the thickness of damage zone in T-peeling tests and the dependence is traced to hysteresis energy, although the origin of such dependence under small-scale inelasticity peel remains unexplained (Yu et al., 2009). The confounding effects due to hysteresis energy mask the basic fact: the dependence of toughness on thickness is correlated with work of fracture. We calculate the work of fracture W_f based on the stress-stretch curves. The average work of fracture is $W_f \sim 1.51 \times 10^5\,\mathrm{J/m^3}$, which is close to the slope of the G-h relation, $\sim 1.87 \times 10^5\,\mathrm{J/m^3}$.

Based on our experimental findings, we rewrite the G-h relation as follows. When the hydrogel thickness h is smaller than the fractocohesive length R_f, the steady peel force is linear in the thickness with a slope of W_f, $G = \Gamma_0 + hW_f$. When the hydrogel thickness h is larger than the fractocohesive length R_f, the steady peel force is independent of the thickness, and plateaus at $\Gamma = \Gamma_0 + R_f W_f$. When the soft materials have large hysteresis, work of fracture is comparable to the hysteresis energy, $W_f \sim W_D$. Also note that, because $\Gamma >> \Gamma_0$, the above relation recovers the definition of the fractocohesive length, $R_f = \Gamma/W_f$.

8. Elastic dissipater

The above modification makes us revisit a basic notion in fracture mechanics. Once again imagine the three material particles, A, B, C, marked near the crack path (Fig. 10a). Also sketched is the stress-stretch curve of a large thin sheet subject to load and unload, where we mark three states of the sheet, also labeled by A, B, C (Fig. 10b). The loading and unloading curves define two areas: the elastic energy W_E, and the hysteresis energy W_D. It is commonly believed that the three particles near the crack path correspond to the three states on the stress-stretch curve, and that only the hysteresis energy W_D contributes to toughness. Our experimental data suggest that this notion is wrong for our experiments here. Rather, at point B, the work by the machine is the whole area under the loading curve, i.e. work of fracture W_f. As the crack propagates, the entire work of fracture W_f is released. This process is similar to a common but often unheeded experimental fact. When a large sheet of hydrogel is stretched to rupture into two pieces, all the work applied during loading is released.

When the hysteresis energy is much larger than the elastic energy, $W_D >> W_E$, the material exhibits hysteresis-dominant toughening. When the hysteresis energy is much smaller than the elastic energy, $W_D << W_E$, the material exhibits elasticity-dominant toughening. Familiar materials of hysteresis-dominant toughening include metals, plastics, double-network hydrogels, as well as elastomers of high viscosity, strain-induced crystallization, and inorganic reinforcement. Materials of elasticity-dominant toughening, however, have not received comparable attention, but one sees numerous examples once the principle is identified. The data reported here shows that the polyacrylamide hydrogel is a material of elasticity-dominant toughening.

We may as well trace materials of elasticity-dominant toughening back to the classical Lake-Thomas model (Lake and Thomas, 1967). At the crack front, just before a polymer chain breaks, all covalent bonds in the polymer chain are stretched near the breaking point. The rupture of the polymer chain dissipates the elastic energy stored in all the covalent bonds in the polymer chain, even though only one bond breaks. The elasticity-dominant toughening comes from the enormous difference in strength between the covalent bonds along each polymer chain and the noncovalent bonds between the polymer chains. The weak noncovalent bonds deconcentrate stress, so that the entire polymer chain carries a high stress before rupture, and dissipates the energy stored in the entire chain upon rupture. That is, the weak noncovalent bonds make an individual polymer chain the elastic dissipater, instead of an individual covalent bond. It is the weakness of the nonviolent bonds that enlarges the elastic dissipater and toughens the elastomer. A crack advances in a polymer network by releasing the covalent energy of a layer of polymer chains. By contrast, in the Griffith model for a silica glass (Griffith, 1921), the covalent bonds do

not form polymer chains, and an individual covalent bond is the elastic dissipater. A crack advances in the glass by releasing the covalent energy of a layer of atoms. It is the high strength of the covalent bonds that limits the elastic dissipater to an individual covalent bond.

The elasticity-dominant toughening has been used recently to design stretchable materials of high toughness and low hysteresis (Wang et al., 2019). Such a material is a composite of two stretchable materials. The compliant matrix deconcentrates the stress in the stiff fibers at the crack front, and elastically stores the energy over long segments of the fibers. As the crack advances, the fibers break. The release of the elastic energy stored in the fibers contributes to the high toughness of the composite. It is the softness of the matrix that enlarges the elastic dissipater to an individual fiber, or at least to a long segment of the fiber. As noted in (Wang et al., 2019), the elasticity-dominant toughening prevails in many heterogeneous materials, including elastic lattices of hard materials (Tankasala et al., 2015).

A far-reaching consequence of elastic dissipater is to create materials of exceptionally high fatigue threshold, a direction of research that we have started recently (Xiang et al., 2019).

We now generalize the Lake-Thomas model to account for several experimental findings of Paper I and this paper. (1) Under broad conditions, the polyacrylamide hydrogel is nearly elastic, with negligible time-dependent inelasticity. (2) When a large sheet of the hydrogel is stretched to a point near rupture, only a small fraction of polymer chains break, leading to narrow hysteresis, $W_D << W_E$. Thus, the work of fracture, $W_f = W_D + W_E$, mostly comes from the release of the elastic energy W_E, rather than the hysteresis energy W_D. (3) In peeling the hydrogel, the linear range of the G-h relation has the slope comparable to the work of fracture, W_f.

The classical Lake-Thomas model releases the elastic energy of a single layer of polymer chains. Our experimental findings motivate us to generalize the Lake-Thomas model. A crack not only cuts a layer of polymer chains on the crack plane, but also breaks some polymer chains in a zone of thickness of the fractocohesive length. Even though only a small fraction of the chains in the zone rupture, all the elastic energy stored in this zone contributes to toughness. The large fractocohesive length deconcentrates stress at the crack front. The stress-stretch state in the fracture process zone is comparable to that corresponding to the work of fracture, W_f. The toughness of the hydrogel, $\Gamma = \Gamma_0 + R_f W_f$, comes from a synergy of two toughening mechanisms: the covalent energy in the polymer chains that bridge the crack, and the work of fracture in a zone of the thickness of the fractocohesive length. In the generalized Lake-Thomas model, the elastic dissipater is no longer an individual polymer chain, but the entire zone of the thickness of the fractocohesive length. Both toughening mechanisms—the bridging polymer chains and the fracture process zone—are elasticity-dominant.

9. Conclusion

In summary, we test the hypothesis of elastic dissipater by peeling a polyacrylamide hydrogel of various thicknesses. The relation between the steady peel force and the hydrogel thickness is characterized by four quantities: the peel threshold, toughness, work of fracture, and transition thickness. The peel threshold is a convenient proxy for the fatigue threshold. All the energy stored in the fracture process zone contributes to toughness, even though only a small fraction of the polymer chains in the fracture process zone rupture. Elastic dissipater is a potent mechanism to create materials of high toughness, high threshold, and low hysteresis.

Acknowledgments

This work at Harvard is supported by the NSF MRSEC (DMR-1420570). J. Liu, T. Yin, and S. Qu are grateful of the support by the National Natural Science Foundation of China (Nos, 11525210, 11621062, 91748209). J. Liu and T. Yin are supported by the China Scholarship Council as visiting scholars at Harvard University.

References

Aubrey, D., Welding, G., Wong, T., 1969. Failure mechanisms in peeling of pressure-sensitive adhesive tape. J. Appl. Polym. Sci. 13, 2193–2207.
Bai, R., Chen, B., Yang, J., Suo, Z., 2019a. Tearing a hydrogel of complex rheology. J. Mech. Phys. Solids 125, 749–761.
Bai, R., Yang, J., Suo, Z., 2019b. Fatigue of hydrogels. Eur. J. Mech. A/Solids 74, 337–370.
Bai, R., Yang, Q., Tang, J., Morelle, X.P., Vlassak, J., Suo, Z., 2017. Fatigue fracture of tough hydrogels. Extrem. Mech. Lett. 15, 91–96.
Chen, C., Wang, Z., Suo, Z., 2017. Flaw sensitivity of highly stretchable materials. Extrem. Mech. Lett. 10, 50–57.
Creton, C., 2017. 50th anniversary perspective: networks and gels: soft but dynamic and tough. Macromolecules 50, 8297–8316.
Creton, C., Ciccotti, M., 2016. Fracture and adhesion of soft materials: a review. Rep. Prog. Phys. 79, 046601.
Gardon, J.L., 1963. Peel adhesion. I. Some phenomenological aspects of the test. J. Appl. Polym. Sci. 7, 625–641.
Gent, A., 1974. Fracture mechanics of adhesive bonds. Rubber Chem. Technol. 47, 202–212.
Gent, A., Petrich, R., 1969. Adhesion of viscoelastic materials to rigid substrates. Proc. R. Soc. Lond. A. Math. Phys. Sci. 310, 433–448.
Gent, A.N., Hamed, G.R., 1977. Peel mechanics of adhesive joints. Polym. Eng. Sci. 17, 462–466.
Gong, J.P., 2010. Why are double network hydrogels so tough? Soft. Matter 6, 2583–2590.
Gong, J.P., Katsuyama, Y., Kurokawa, T., Osada, Y., 2003. Double-network hydrogels with extremely high mechanical strength. Adv. Mater. 15, 1155–1158.
Greensmith, H.W., Thomas, A., 1955. Rupture of rubber. III. Determination of tear properties. J. Polym. Sci. 18, 189–200.
Griffith, A.A., 1921. The phenomena of rupture and flow in solids. Philos. Trans. R. Soc. S-A 221, 163–198.
Igarashi, T., 1975. Mechanics of peeling of rubbery materials. I. Peel strength and energy dissipation. J. Polym. Sci. B. Polym. Phys. 13, 2129–2134.
Irwin, G., 1948. Fracturing of Metals, 147. ASM, Cleveland 19–19.
Kalcioglu, Z.I., Mahmoodian, R., Hu, Y., Suo, Z., Van Vliet, K.J., 2012. From macro-to microscale poroelastic characterization of polymeric hydrogels via indentation. Soft. Matter 8, 3393–3398.
Kundu, S., Crosby, A.J., 2009. Cavitation and fracture behavior of polyacrylamide hydrogels. Soft. Matter 5, 3963–3968.

Lake, G., Thomas, A., 1967. The strength of highly elastic materials. Proc. R. Soc. Lon. 300, 108–119.
Long, R., Hui, C.-Y., 2015. Crack tip fields in soft elastic solids subjected to large quasi-static deformation—a review. Extrem. Mech. Lett. 4, 131–155.
Long, R., Hui, C.-Y., 2016. Fracture toughness of hydrogels: measurement and interpretation. Soft. Matter 12, 8069–8086.
Luo, Y.-R., 2007. Comprehensive Handbook of Chemical Bond Energies. CRC press.
Mao, Y., Talamini, B., Anand, L., 2017. Rupture of polymers by chain scission. Extrem. Mech. Lett. 13, 17–24.
Mao, Y., Anand, L., 2018. A theory for fracture of polymeric gels. J. Mech. Phys. Solids 115, 30–53.
Naassaoui, I., Ronsin, O., Baumberger, T., 2018. A poroelastic signature of the dry/wet state of a crack tip propagating steadily in a physical hydrogel. Extrem. Mech. Lett. 22, 8–12.
Noselli, G., Lucantonio, A., McMeeking, R.M., DeSimone, A., 2016. Poroelastic toughening in polymer gels: a theoretical and numerical study. J. Mech. Phys. Solids 94, 33–46.
Orowan, E., 1950. Fatigue and Fracture of Metals. Symposium at massachusetts institute of technology.
Rivlin, R., Thomas, A.G., 1953. Rupture of rubber. I. Characteristic energy for tearing. J. Polym. Sci. 10, 291–318.
Sun, J.-Y., Zhao, X., Illeperuma, W.R., Chaudhuri, O., Oh, K.H., Mooney, D.J., Vlassak, J.J., Suo, Z., 2012. Highly stretchable and tough hydrogels. Nature 489, 133.
Tanaka, Y., Abe, H., Kurokawa, T., Furukawa, H., Gong, J.P., 2009. First observation of stick−slip instability in tearing of poly (vinyl alcohol) gel sheets. Macromolecules 42, 5425–5426.
Tang, J., Li, J., Vlassak, J.J., Suo, Z., 2017. Fatigue fracture of hydrogels. Extrem. Mech. Lett. 10, 24–31.
Tankasala, H., Deshpande, V.S., Fleck, N.A., 2015. 2013 Koiter medal paper: crack-tip fields and toughness of two-dimensional elastoplastic lattices. J. Appl. Mech. 82, 091004.
Wang, X., Hong, W., 2012. Delayed fracture in gels. Soft. Matter 8, 8171–8178.
Wang, Z., Xiang, C., Yao, X., Le Floch, P., Mendez, J., Suo, Z., 2019. Stretchable materials of high toughness and low hysteresis. Proc. Natl. Acad. Sci. U S A 116, 5967–5972.
Webb, T., Alfantis, E., 1995. Oscillatory fracture in polymeric materials. Int. J. Solids Struct. 32, 2725–2743.
Xiang, C., Wang, Z., Yang, C., Yao, X., Wang, Y., Suo, Z., 2019. Stretchable and fatigue-resistant materials. Unpublished.
Yang, C., Yin, T., Suo, Z., 2019. Polyacrylamide hydrogels. I. Network imperfection. J. Mech. Phys. Solids 131, 43–55.
Yu, Q.M., Tanaka, Y., Furukawa, H., Kurokawa, T., Gong, J.P., 2009. Direct observation of damage zone around crack tips in double-network gels. Macromolecules 42, 3852–3855.
Yu, Y., Landis, C.M., Huang, R., 2018. Steady-state crack growth in polymer gels: a linear poroelastic analysis. J. Mech. Phys. Solids 118, 15–39.
Yuk, H., Zhang, T., Lin, S., Parada, G.A., Zhao, X., 2016. Tough bonding of hydrogels to diverse non-porous surfaces. Nat. Mater. 15, 190.
Zhang, E., Bai, R., Morelle, X.P., Suo, Z., 2018a. Fatigue fracture of nearly elastic hydrogels. Soft. Matter 14, 3563–3571.
Zhang, T., Lin, S., Yuk, H., Zhao, X., 2015. Predicting fracture energies and crack-tip fields of soft tough materials. Extrem. Mech. Lett. 4, 1–8.
Zhang, W., Hu, J., Tang, J., Wang, Z., Wang, J., Lu, T., Suo, Z., 2019. Fracture toughness and fatigue threshold of tough hydrogels. ACS Macro. Lett. 8, 17–23.
Zhang, W., Liu, X., Wang, J., Tang, J., Hu, J., Lu, T., Suo, Z., 2018b. Fatigue of double-network hydrogels. Eng. Fract. Mech. 187, 74–93.
Zhao, X., 2014. Multi-scale multi-mechanism design of tough hydrogels: building dissipation into stretchy networks. Soft. Matter 10, 672–687.
Zhou, Y., Zhang, W., Hu, J., Tang, J., Jin, C., Suo, Z., Lu, T., 2019. The stiffness-threshold conflict in polymer networks and a resolution. Unpublished.